

Article

Energy Transfer and Damage Evolution Process Research of Ore Rock-Filling Body under the Blasting Load

Zijin Xia, Haiping Yuan , Hengzhe Li , Xuyang Yu, Xingye Fang and Songtao Huang

College of Civil Engineering, Hefei University of Technology, Hefei 230009, China

* Correspondence: seapie@hfut.edu.cn

Abstract: The low intensity and frequent blasting shock wave created by a blasting impact will exert notable destructive effects on an ore rock-filling body. In order to investigate the energy transfer process of the blasting shock wave energy in the filling body and the damage evolution process of the filling body, the software PFC^{2D} was used to numerically simulate and monitor the blasting stress curve of the stope and the energy transfer process. In addition, the incident of the pulse wave with the transmission boundary of the filling body was employed to obtain the fitting curve of the stress wave energy. Simultaneously, the language FISH was adopted to realize the two-dimensional visualization of the damage degree. The results indicate that: (i) the upper side of the filling body is accessible to generate energy superposition, and the shock wave is diffused in a waveform. Moreover, a few large and deep cracks are produced in the central area; (ii) during the blasting process, the damaged area extended continuously from the bottom to the top along the boundary surface of an ore rock-filling body and finally diffused to both sides; (iii) the energy attenuation of the stress wave in an ore body roughly performs the distribution of power function. Consequently, the research results can contribute to the safety evaluation of mining engineering using differential blasting technology.

Keywords: differential blasting technology; stress wave; transmission boundary; mining engineering



Citation: Xia, Z.; Yuan, H.; Li, H.; Yu, X.; Fang, X.; Huang, S. Energy Transfer and Damage Evolution Process Research of Ore Rock-Filling Body under the Blasting Load. *Minerals* **2022**, *12*, 1362. <https://doi.org/10.3390/min12111362>

Academic Editor: Mamadou Fall

Received: 19 September 2022

Accepted: 25 October 2022

Published: 26 October 2022

Publisher's Note: MDPI stays neutral with regard to jurisdictional claims in published maps and institutional affiliations.



Copyright: © 2022 by the authors. Licensee MDPI, Basel, Switzerland. This article is an open access article distributed under the terms and conditions of the Creative Commons Attribution (CC BY) license (<https://creativecommons.org/licenses/by/4.0/>).

1. Introduction

In recent years, the issue of pillar recovery has been extensively studied by scholars in the mining field. For reasons of maintaining the stability of the goaf on both sides of the pillar in practical engineering, the loose cement material was normally filled in the goaf before blasting and recovering the pillar. Additionally, the blasting vibration generated by explosive activities will cause specific damage to the filling body and even lead to local caving or collapse accidents of the latter. In most cases, the causes of accidents are due to the accumulation and superposition of the energy generated by the sequential blasting of explosives in the stope environment [1]. Therefore, the law of energy transfer and the damage evolution in the ore rock and filling body under the blasting activities remain to be further studied. In order to examine the impacts of differential blasting on the stope environment, domestic and foreign experts have completed numerous research work in this field. To simulate the blasting process by means of the particle flow, which proves to be a common analytical strategy. Chong Shi et al. [2,3] used the particle flow to simulate the propagation law of explosive stress wave in a rock mass and dynamically characterized the failure process of a rock mass. Bingxiang Wang et al. [4] explored the function of the stress wave attenuation of brittle granular particles under shock loads. Xuefeng Li et al. [5] investigated the application of multi-layer differential blasting mining technology in small-scale ore mining. Zhongwen Yue et al. [6–8] concentrated on the mechanism and contributing variables of crack formation between the differential blasting holes.

In addition, Xuebin Guo et al. [9] found that the stress wave generated by differential blasting technology would perform apparent superposition effects after passing a certain distance. Meanwhile, the time interval of differential blasting will also produce heavy

impacts on the blasting effect [10–12]. Two-step stoping blasting is normally involved in mining engineering regarding non-ferrous metals. Additionally, the filling body will be damaged during the process of stoping blasting pillars.

Furthermore, Grady and Kipp put forward the earliest rock-blasting damage model in 1980, model GK [13], followed by model TCK [14] and model KUS [15], which can reflect rock damage under specific blasting dynamic loads in spite of incalculable shortcomings. Thus, Thome [16], Yang [17], Liu [18], Song [19], Wenbo Lu [20], and Jun Yang et al. [21] modified the aforementioned models.

Countless experts and scholars have established a moderately comprehensive theoretical system in differential blasting technology [22–25]. The theoretical analysis of the explosion process [26,27] has momentous reference value for researching dynamic explosion processes, but there are still some points to be improved. For instance, the simulation method for blasting shock waves is limited, and the dynamic boundary condition performs poorly.

In this paper, with respect to the discrete element software PFC^{2D}, the ore body to be mined was employed to conduct the numerical simulation of differential blasting by the filling method, and the half-sine pulse-stress wave and expansion loading method of explosive point particles were embraced to simulate the blasting shock wave in reality. Moreover, the transmission boundary was adopted to reconstruct the practical dynamic boundary environment of the stope. Principally, the influences of the blasting shock wave were explored to make the boundary of the ore body and the filling body. In the meantime, the energy dissipation process of the stress wave among the filling body was discussed as well. Furthermore, an updated idea was provided by the Language FISH for real-time damage monitoring of the filling body in this research. Consequently, the research results are importantly referenced for mining engineering using the filling method of differential blasting and are valuable references to the safety evaluation of surrounding rock in a specific range of stope.

2. Discrete Element Model Theory Assumption

2.1. Expansion Loading Method of Explosive Point Particles

Under the blasting function of the concentrated charges, the shock wave created by blasting diffused around along the radial direction. Indeed, the blasting shock wave was identical to the pulse stress wave by the expansion loading method of explosive point particles. More specifically, the process of the stress wave is relatively complex, from the initiation of blasting to the state of the peak and dissipation, respectively. In addition, the loading method simplifies this complicated process into a roughly simple form of the half-sine wave, in which the duration of the rising stage of blasting stress is equal to that of the falling stage, but this method is only a simplified expression of the blasting stress [3].

The expression and the variation curve of the function $P(t)$ of the explosion stress with time (Figure 1) are depicted as follows:

$$P(t) = \frac{A}{2} \left(1 - \cos\left(\frac{2\pi}{\Delta T} t\right) \right) \quad (1)$$

where A represents the impact stress caused by the explosion, ΔT is the action time of the pulse stress wave, t signifies the explosion duration, and $p(t)$ denotes the stress generated by the explosion.

In engineering, the charging methods of the blast holes can be divided into coupling charging and decoupling charging. By and large, the coupling charging implies that there is no gap between the explosives and the wall of blast holes so as to decrease the impact of voids on the blasting effect. Compared with the decoupling charging, a faster stress decay rate can be examined in the coupling charging, and the vast majority of the energy is absorbed by the ore body around the blast holes. In addition, the ore body around the blast holes performs a higher degree of fragmentation and lower bulk percentage, which is convenient for mining and effectively reduces the expenses of extraction.

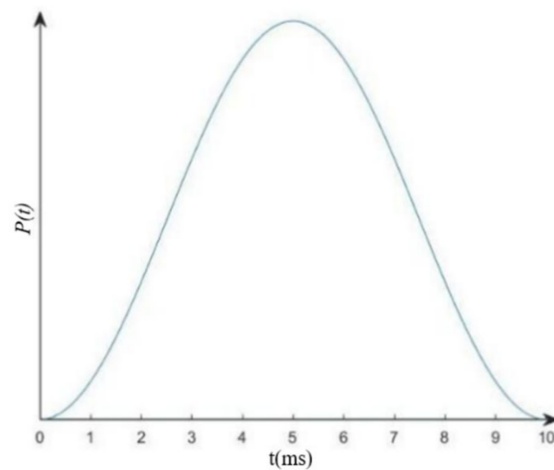


Figure 1. Stress wave curve with time.

The Impact pressure on the wall of blast holes during coupling charging can be expressed as follows [3]:

$$P_2 = P_c \frac{2}{1 + \rho_0 D / \rho_{r0} c_p} \tag{2}$$

where ρ_0 represents the density of the explosives, ρ_{r0} denotes the density of rock, c_p is the longitudinal wave velocity, D signifies the detonation velocity of the explosives, and P_c is the surface pressure of the explosion wave.

Admittedly, the blasting load in PFC^{2D} was realized by the expansion effect of the explosive point particles; that is, the expansion loading method of the explosive point particles. By virtue of controlling the radius of the explosive point particles, the amount of overlap between the explosive point particles and the particles of the surrounding ore body was generated until the explosive point particles expanded to the outer edge of the blasting cavity. As a matter of fact, the ore body particles would be endowed with specific stiffness before the explosion, within which the expansion range of the original charges would produce a certain amount of compression so as to simulate the stress wave created by the explosion from the blast points.

In brief, the ratio between the radius of the blasting cavity and the radius of the explosive point particles is called the blasting expansion ratio, and the larger the blasting expansion ratio, the higher the achieved explosive intensity. The schematic diagram of the blasting principle is exhibited in Figure 2.

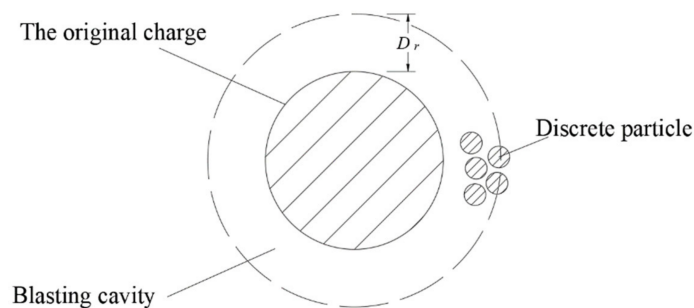


Figure 2. Schematic diagram of blasting principle.

It is assumed that the radius of the original charges was r_0 . When the radius expands to the radius of the blasting cavity, the pressure p_2 acting on the rock wall would generate radial thrust on the surrounding rock particles. Assuming the particle stiffness of the ore body represents K_n , the resultant thrust force was $F = K_n d_r = 2\pi r_0 p_2$. Under the

conditions of contact stiffness and explosion pressure, the formula of the variation peak of the radius of the explosion particles d_r can be expressed as follows:

$$d_r = \frac{2\pi r_0 p_2}{K_n} \tag{3}$$

Additionally, a concentrated blasting point was buried in the rock mass, and the explosives were detonated by the mentioned blasting principle, and the obtained particle velocity cloud diagram can be displayed in Figure 3. Accordingly, the shock wave resulted from blasting diffused around, and the simulation results were consistent with the theory. As a result, to a certain extent, a larger instantaneous velocity was generated in a certain range of particles, which reconstructed the impact of the concentrated blasting points in the rock mass on the surrounding particles.

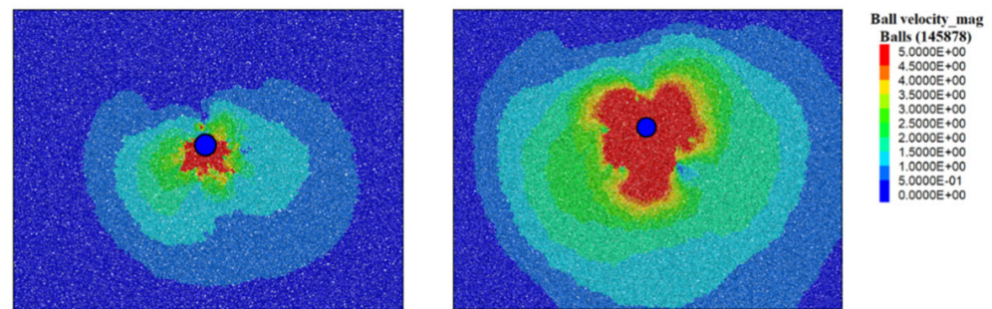


Figure 3. Blasting effects of concentrated blasting points.

2.2. Transmission Boundary

Through the blasting numerical simulation, when the blasting stress wave reaches the boundary of the model, it will generate reflected waves on the boundary surface of the model, which will disturb the already established blasting stress field. Generally, this phenomenon is defined as the boundary reflection effect. During practical engineering, the energy formed by the explosion of the blast points will propagate into infinity. Under the function of rock-mass damping, the energy will gradually dissipate. Furthermore, a part of the energy caused by the production of the boundary reflection effect will propagate back, which will cancel each other out with the stress wave continuously generated by blasting so that the numerical simulation results are extremely different from reality.

In order to eliminate the boundary effect of the model, the software PFC was adopted to extract the unbalanced force, and a reverse load was applied to the boundary particles, respectively. The value of the reverse load is equal to the unbalanced forces so as to absorb the incident wave energy. The mechanism of this dynamic boundary condition, the transmission boundary, is shown in Figure 4.

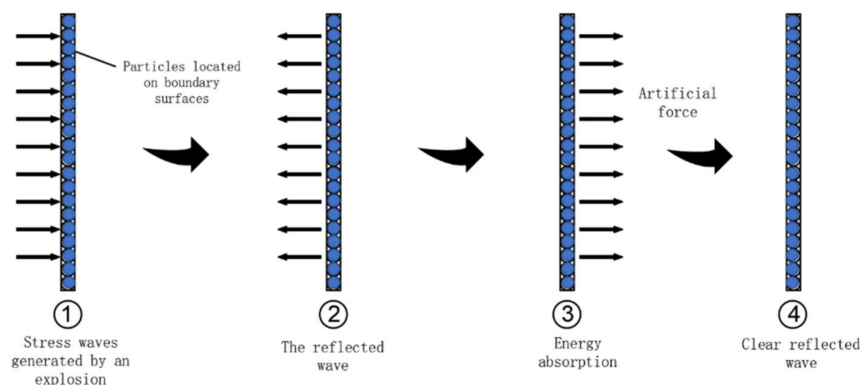


Figure 4. Transmission boundary diagram.

2.3. Selection Principle of Differential Blasting Time Delay

In engineering, there are two kinds of initiation modes: simultaneous porous initiation and delayed porous initiation (differential blasting). Alternatively, practice demonstrates that differential blasting technology can adequately enhance the blasting effect of explosives, and the blasting points can produce a flying plane in turn, which is beneficial to the fall of the crushed ore and vastly decrease the bulk rate so that the blasting effect can perform more favorably.

Indeed, the time interval selection used in differential blasting technology is the predominant factor for determining the blasting effect. In addition, the development process of blasting dynamics has led to innumerable theories that are relevant to determining the optimal blasting time interval. For instance, the scientist of the association of the Soviet Union, Levski, proposed that under the condition of an optimal blasting time interval, the stress wave generated by the adjacent blasting points shall be in the best superposition state [28]. After an enormous number of practical blasting cases, the differential blasting time interval model can be determined as follows [28]:

$$T = \frac{a}{V_p} + 5 \times 10^{-4} \times \sqrt{Q} \tag{4}$$

where T denotes the differential time interval, a represents the distance between the blasting holes, Q stands for the charging capacity, and V_p signifies the propagation velocity of the incident stress wave.

3. Effect Evaluation of Differential Blasting of Ore Body Beneath Transmission Boundary

3.1. Introduction to Basic Engineering Conditions

To illustrate, a certain area to be mined in one mine in East China, whose both sides had been worked out. For this reason, the differential blasting method was adopted to conduct the blasting mining of the intermediate mining area. In order to reduce the disturbance of the surrounding rock due to blasting and decrease the risk of detonation, the particles were employed to backfill and grout, filling the pore of the goaf on both sides before the explosion so that the huge impact caused by blasting in the middle part could be absorbed. The specific backfilling process is shown in Figure 5. After backfilling the goaf, the mining body to be excavated, 1.5 m, was used as the clearance area in advance so that the debris fell and piled up after the explosion.

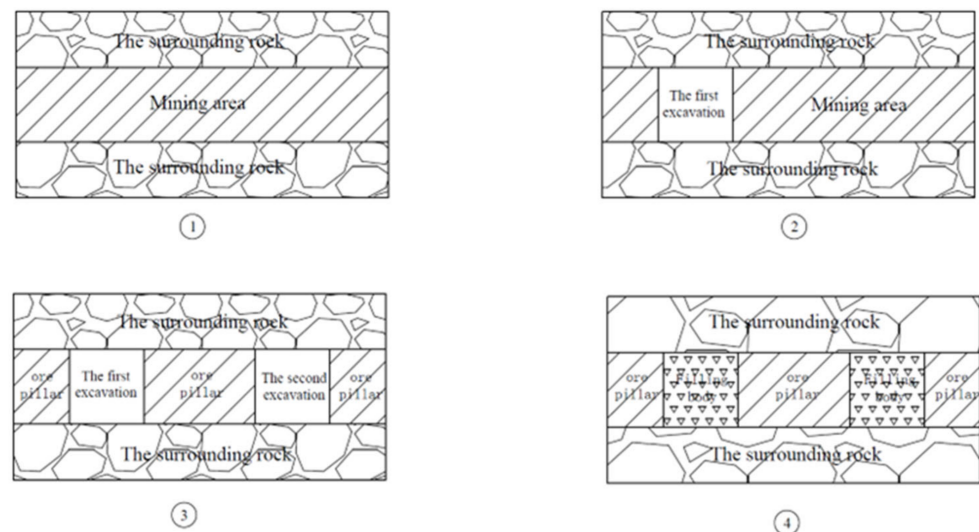


Figure 5. Section layout of ore body.

Particularly, a rectangular layout of five rows and three columns was adopted for the blasting holes, whose charging holes on both sides were 2 m away from the boundary surface of the filling body and the ore body. In addition, the longitudinal and transverse spacing of the charging holes were 1.5 m and 3 m, respectively. Furthermore, the explosion delay of the blasting hole lasted 10 ms. In fact, the identical blasting hole was detonated at the same time, and the explosive time interval of the two adjacent rows of the blasting holes was 5 ms.

Hence, the ore body section layout in the discrete element model is displayed in Figure 6. The parameters of the filling body and the ore body and the parameters of the blasting holes are exhibited in Tables 1–5, respectively.

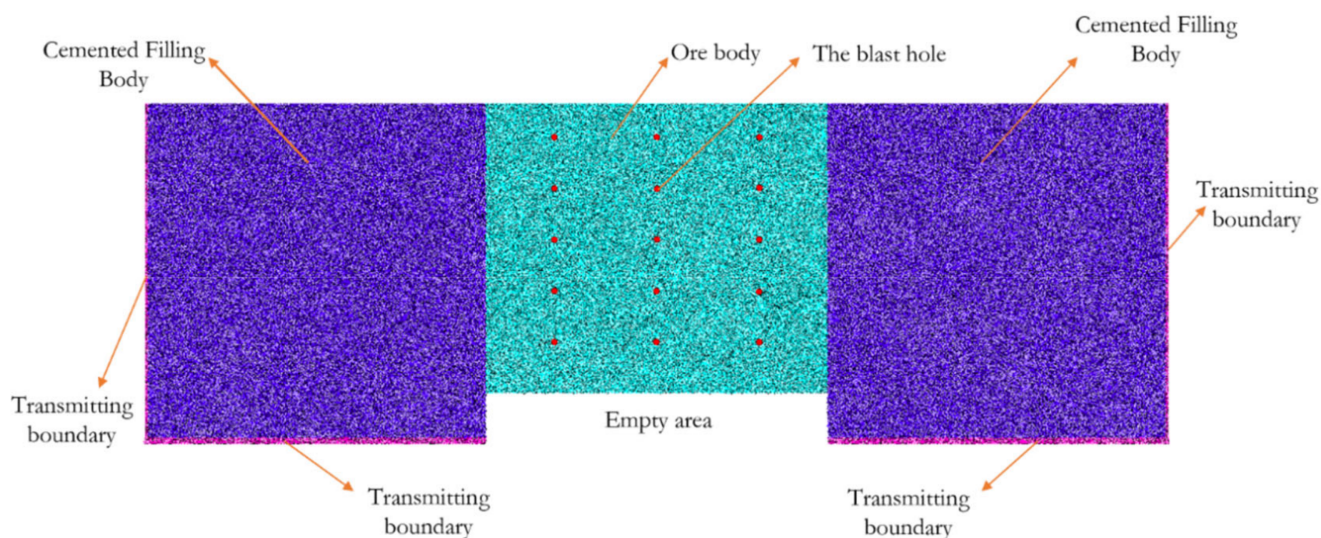


Figure 6. Section layout of the ore body.

Table 1. Physical and mechanical calculation parameters of ore and rock.

Density (kg/m ³)	Tensile Strength (MPa)	Compressive Strength (MPa)	Possion's Ratio	Cohesion (MPa)	Internal Friction Angle (°)
3000	13.13	80.85	0.305	6.551	31.99

Table 2. Physical and mechanical calculation parameters of filling body.

Density (kg/m ³)	Tensile Strength (MPa)	Compressive Strength (MPa)	Possion's Ratio	Cohesion (MPa)	Internal Friction Angle (°)
2000	0.35	3.6	0.2	1.55	30

Table 3. Table of mesoscopic parameters of filling body.

Particle Parameters	Value	Bond Parameters	Value
Minimum particle radius/m	0.0050	Pb_emod	4.5×10^{10} Pa
Maximum particle radius/m	0.0075	Pb_kratio	3.0
Grain density/kg/m ³	2000	Pb_ten	4.5×10^{10} Pa
Damping ratio	0.7/0.5	Pb_coh	1×10^8 Pa
Friction coefficient	0.5	Kratio	3.0

Table 4. Table of mesoscopic parameters of ore body.

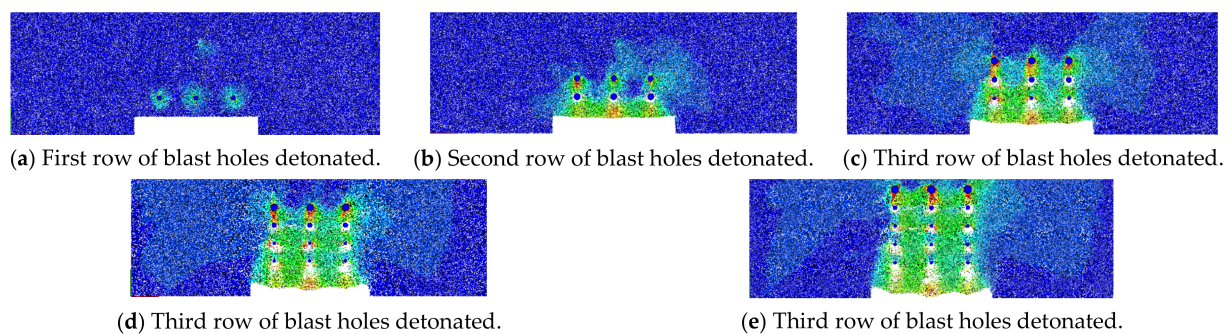
Particle Parameters	Value	Bond Parameters	Value
Minimum particle radius/m	0.0050	Pb_emod	5.0×10^{10} Pa
Maximum particle radius/m	0.0075	Pb_kratio	3.0
Grain density/kg/m ³	3000	Pb_ten	5.0×10^{10} Pa
Damping ratio	0.7/0.5	Pb_coh	3.75×10^8 Pa
Friction coefficient	0.8	Kratio	3.0

Table 5. Table of parameters of blasting holes.

Blasting Hole Parameters	Value	Blasting Hole Parameters	Value
Blasting hole radius/m	0.15	Pb_emod	5.0×10^{10} Pa
Blasting radius expansion ratio	2.5	Pb_kratio	3.0
Peak value of explosive stress/Pa	5.0×10^7	Kratio	3.0

3.2. Numerical Simulation of Differential Blasting

In this study, the mentioned conditions were numerically simulated by using the discrete element software PFC^{2D}. In the first place, the transmitted boundary was adopted to eliminate the reflected waves on the boundary surface, and then the expansion loading method was employed for the explosive points to simulate the stress wave effect produced by the real blasting with discrete elements. By means of controlling the time when the radius of the blasting points began to expand, the blasting results of the two adjacent rows of the blasting points were orderly realized (Figure 7).

**Figure 7.** Differential blasting process diagram.

After differential blasting in the area to be mined, the ore body failed under the function of explosion stress, and the particles of the ore body were highly fragmented. From the velocity cloud diagram, it can be easily seen that the blasting funnel formed at the blasting point after the initiation of the explosion. Due to the presence of the volley area, the slag fell successively to it in a funnel shape under the influence of gravity. Since the blasting shock wave would not dissipate the first time after the explosion at the blasting point, the function time of the shock wave would last for a certain while, and the residual energy would still be extensively influential on the filling body after the detonation. Thus, the model was calculated to 10 ms after the explosion of the last row of blasting holes, and the blasting effect diagram could be obtained (Figure 8).

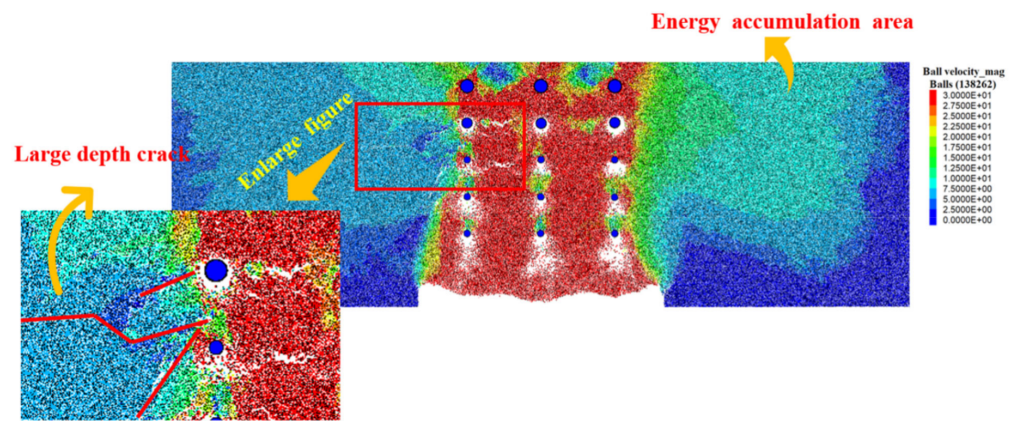


Figure 8. Sketch of blasting effects.

Under the function of enormous impact force, large cracks emerged at the boundary between the filling body and the ore body. In addition, a couple of cracks expand deeper along the direction of the longitudinal wave, and the particles at the interface appear to be crushed. In fact, the energy after the explosion became transitive, and the shock wave would spread radially around. It is not hard to find from Figure 7 that the shock wave induced by each explosion could not dissipate during a short time; on top of that, the evident superposition effect appeared on both sides of the area, especially upon the upper part, where the particles generated a larger instantaneous velocity.

In order to explore the influences of blasting on the particles near the interface, 10 monitoring points were arranged near the boundary along the longitudinal and transverse lines, respectively, with a longitudinal spacing of 1.5 m and a horizontal spacing of equal difference value.

As a result, the arrangement of the monitoring points is displayed in Figure 9. Furthermore, PFC^{2D} was used to monitor the explosion stress at the monitoring points, and the curve of explosion stress with time was finally acquired, as shown in Figure 10.

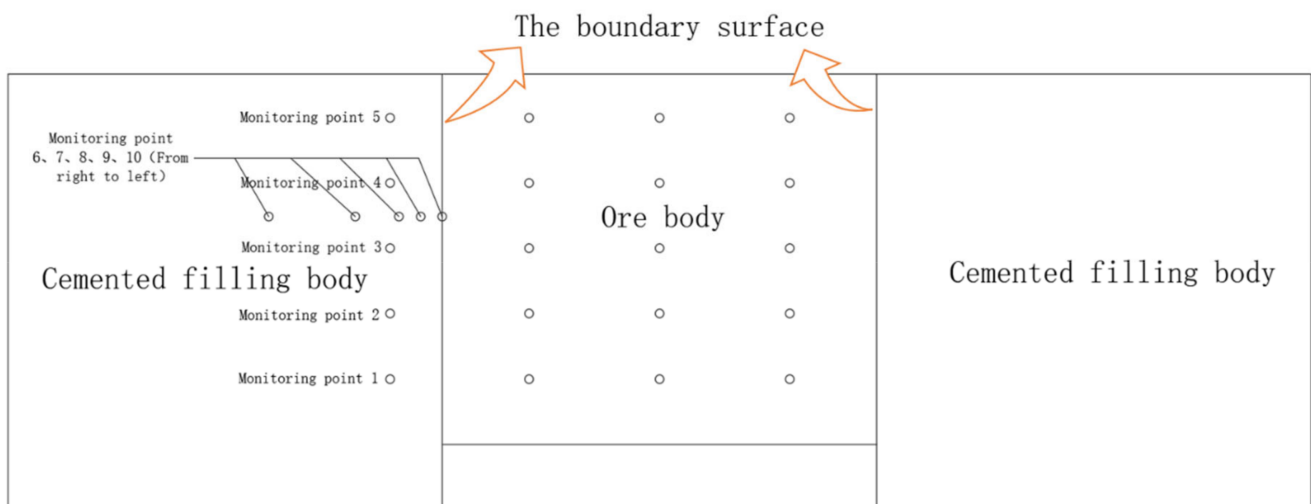


Figure 9. Layout diagram of monitoring points.

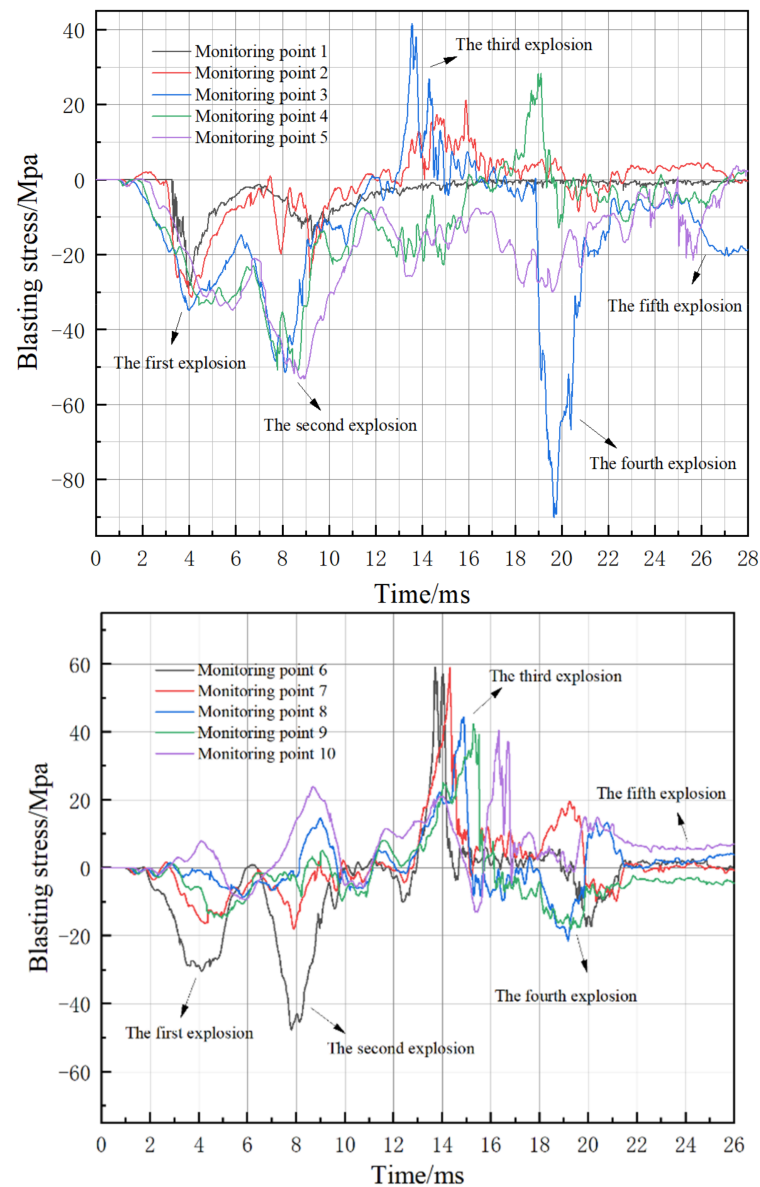


Figure 10. Explosion stress monitoring curve.

According to the explosion stress monitoring curve, it is expedient to know that with the sequential initiation of each row of blasting points, the observing point was subjected to the firm blasting stress, and an irregular fluctuation trend was presented on the monitoring point. Nonetheless, the peak stress point appeared in the curve during the time of initiation instant of each explosion point. Specifically, the blasting stress of the upper monitoring point was commonly more prominent than that of the lower one due to the effects of shock wave propagation and superposition on the top side.

In other words, the middle observing point was exposed to the combined effects of the upper and lower blasting impact forces of the monitoring point. Thus, when the fourth row of the explosion holes exploded, the peak stress of monitoring point 3 would exceed 80 MPa. In comparison, the maximum peak stress of transverse monitoring points 6 and 7, which were close to the middle area of the interface, reached 60 MPa after the detonation of the hole, respectively. In simpler terms, the intense, instantaneous impact stress should be the essential justification for cracks with a deeper depth in the middle part of the filling body.

4. Two-Dimensional Damage Visualization of the Ore Rock-Filling Body Boundary Surface

As a matter of fact, the stress wave generated by blasting activities causes certain damaging effects on the boundary surface of the ore rock-filling body, and the medium in a certain range near the interface will deliver a mechanical response under the mining dynamic behavior. The degree of damage to the filling body will gradually increase with the progression of blasting activities, and the damaged area will also show a certain regularity. Therefore, it has important practical engineering significance to realize the two-dimensional visualization of the degree of damage and evolution process of the ore rock-filling body boundary surface.

In this study, the degree of damage to the contact between the particles in PFC^{2D} was adopted to measure the damage status of the filling body, and the broken contact between the particles was represented using images by the program FISH so as to realize two-dimensional damage visualization.

A program through modeled real-time monitoring has become the primary operating principle of the contact state between all of the particles and constantly traverses all of the contact states between the particles so that the present damage status of the filling body can be evaluated. When the program was employed to recognize the contact in a state of failure, it will automatically generate a labeled line along the normal direction of the wire in the center of the adjacent particles to represent the current location of the damage degree of sets, namely, the denser the lines, the more severe the damage in this area.

As a result, the principle of the schematic can be vividly seen in Figure 11. Accordingly, the contact changes between the ore rock-filling body during the blasting activities can be dynamically characterized by the two-dimensional damage visualization program of the boundary surface of the ore rock-filling body. To a certain extent, the mechanical response process of the filling body can be revealed (as exhibited in Figure 12).

In practical blasting engineering, this technology can be used to predict the impact of blasting activities on the surrounding environment. Meanwhile, the damage evolution process and mechanical response of the filling body through the explosive process can be intuitively perceived.

In this study, the degree of damage to the filling body was monitored within a certain time after initiation, and the existing technical means were adopted to output the images. Thereinto, the marked density in Figure 11 denotes the degree of damage to this area. According to the results of the two-dimensional images (Figure 12a), it is not difficult to observe that massive damage will occur in the circular area of the ore rock centered at the blasting point with the progress of blasting activities, and channels easily form between the blasting points. In addition, the degree of damage to the interface between the middle part of the ore rock area and the filling body on both sides was relatively higher. During the early stage of blasting, the variation in the number of fractures between the particles of the filling body is obvious, as exhibited in Figure 12b. When the blasting progresses to the later phase, the damage will occur in more than 80% of the filling body area, and the damage depths will gradually extend from the position of the boundary surface of the ore rock-filling body to the model boundary.

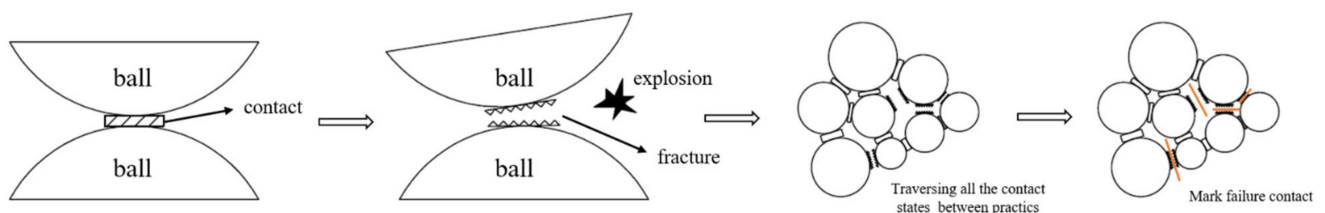
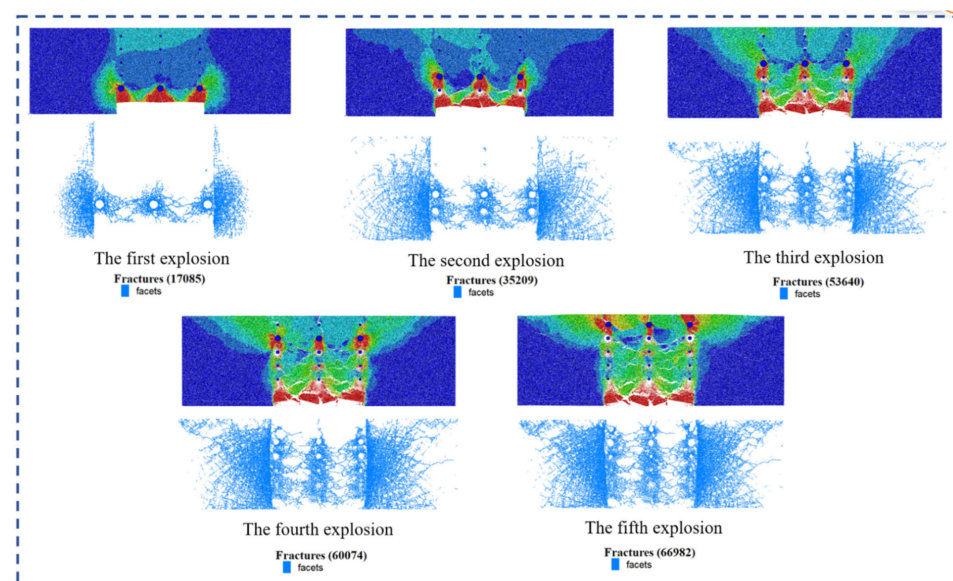
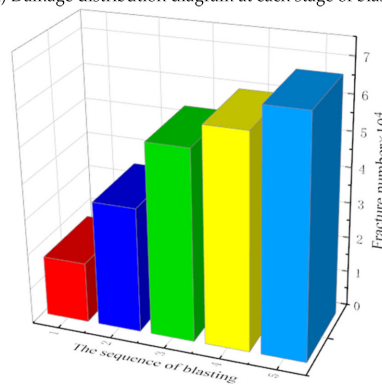


Figure 11. Schematic diagram of damage display principle.



(a) Damage distribution diagram at each stage of blasting



(b) Schematic of the number of cracks generated at each stage of blasting

Figure 12. Evolution process of backfill damage.

In a word, the damage evolution process of the filling body has displayed notable regularity: (i) the filling body that is at the same height as the blasting points will be destroyed promptly after the explosion, and the degree of damage manifests vaguely higher; (ii) the damage on the boundary surface of the ore rock-filling body exhibits a continuous trend of bottom–top expansion. On account of the interface of the ore rock-filling body, which belongs to the junction of two kinds of materials, the strength there behaves roughly weaker, and the distance between the boundary surface and the blasting points performs relatively closer. Thus, it is easier to be damaged under the function of the large instantaneous load. With the increase in the number of explosions, the blasting shock wave will be continuously accumulated and superposed in the filling body, resulting in a large range of damage in the filling body after a detonation of 15 ms.

5. Exploration on Stress Wave Attenuation Law

Admittedly, the shock wave induced by the explosion will propagate in all directions. With the increment of the propagation distance, the energy of the shock wave would be absorbed by the propagating medium due to the damping effect on it and finally dissipated. After the explosion of the blast points, the stress wave would be transmitted to the filling body, whose particles would vibrate in the horizontal direction, which is the result of the function of the longitudinal wave.

To examine the transmission attenuation rule of the explosive stress wave in the filling body after blasting, a set of stress wave pulses was employed to pass through the filling material. Restricted by the number of particles used in the discrete element software,

it could only establish a limited boundary model for numerical simulation. In order to eliminate the boundary reflection wave effect and achieve the maximum restoration of attenuation law that the stress wave travels to infinity, a transmission boundary was applied to the boundary particles of the model to eliminate the influence of the reflected waves on the horizontal vibration of particles. Therefore, the model diagram can be displayed in Figure 13.



Figure 13. Model diagram.

Ten observation points were arranged longitudinally in the middle part of the filling body to monitor the vibration velocity along the horizontal direction of the particles. Since the velocity dispersion of one single particle performed larger in the discrete element software, a measuring circle was introduced into the model. By virtue of monitoring the horizontal velocities of all the particles within the radius of 0.1 m with the measuring point as the center of the circle, the average horizontal velocity value was calculated as the observation point. Hence, a set of pulse stress waves was monitored from incident to ejection for 100 ms. The propagation time of the stress wave from one side of the backfill to the other side was 10 ms (Figure 14), and the monitoring curves of the horizontal velocities along the longitudinal wave direction of the observation points were obtained (Figures 15 and 16).

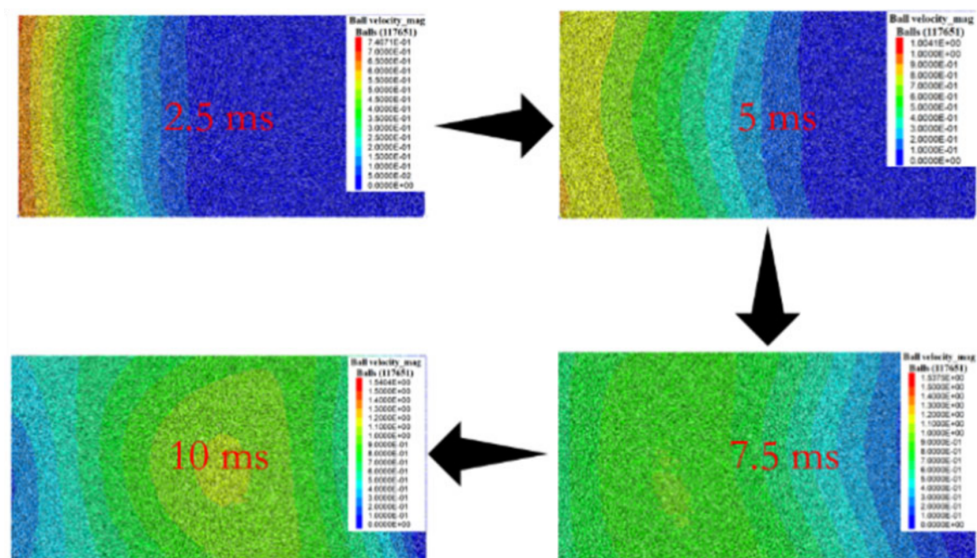


Figure 14. Stress wave propagation process diagram.

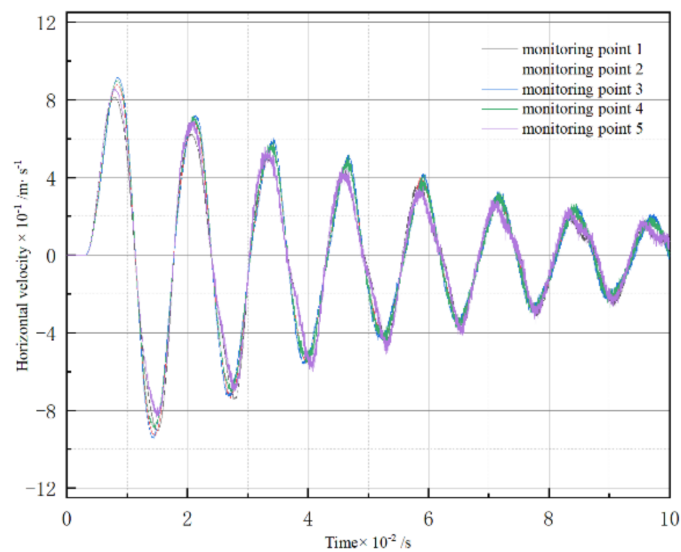


Figure 15. Monitoring curve of horizontal velocities (1).

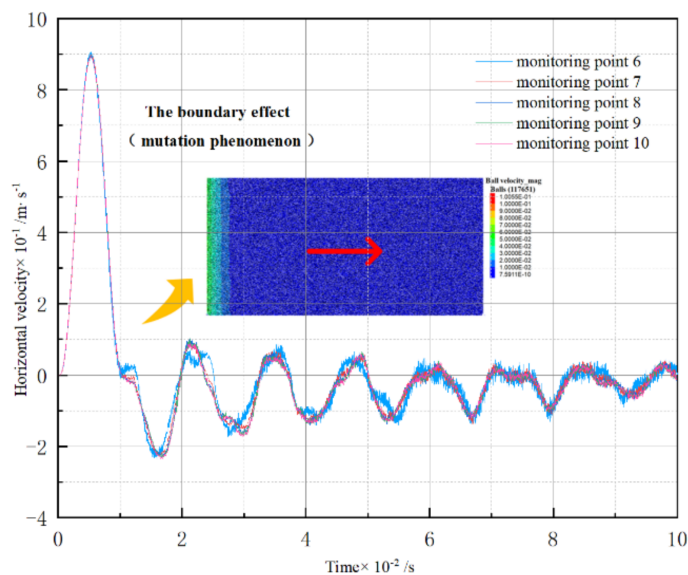


Figure 16. Monitoring curve of horizontal velocities (2).

By means of monitoring the horizontal velocities of the particles in the middle part of the propagation medium, it can be found that the attenuation of the kinetic energy of the particles reveals a confirmed regularity. The damping effect of the medium on particle vibration is obvious. In other words, the velocities generated by the particles under the function of the pulse stress wave will gradually decay, and the amplitude of the particles will increasingly weaken. The points of the peak stress on the monitoring curve were extracted and fitted to obtain the fitting function curve, as shown in Figure 17.

As a consequence, the attenuation values of the peak horizontal velocities of the monitoring points gradually decline with the increment of time, and the curve progressively becomes delicate. The fitted curve satisfies the power function equation $y = ax^b$. The size of the coefficient 'a' is related to the setting of the basic parameters of the model, including the positions of the monitoring points, the wave velocities of the incident wave, the damping effects of the filling body, etc., while the larger the absolute value of the coefficient 'b' is, the faster the horizontal decay velocities of the particles.

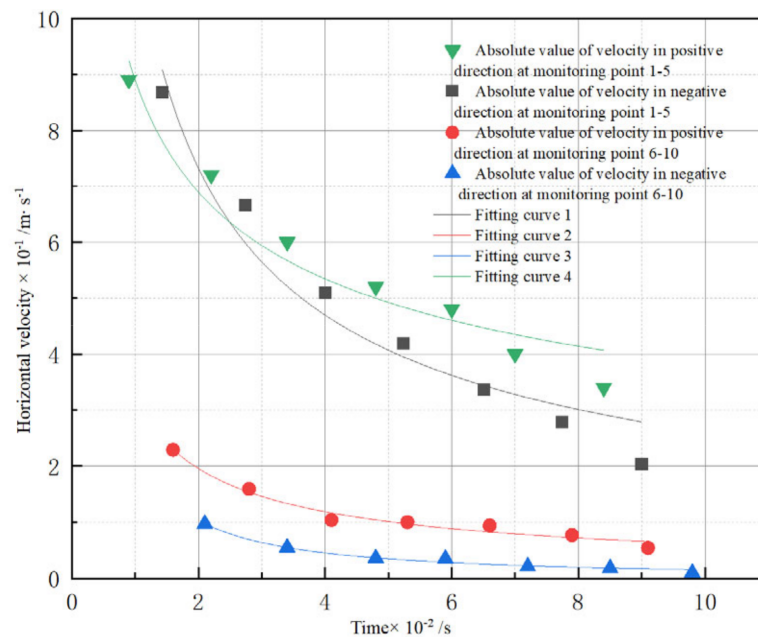


Figure 17. Fitting curve.

In fact, the longer the distance from the observation point to the pulse wave emission source is, the more intense the regularity of the velocity monitoring curve, the more regular a curve "water ripple", and the smoother the fitting curve of decay with time of the particle kinetic energy.

6. Conclusions

(1) During the blasting mining process of a pillar, the blasting shock wave is convenient for generating the superposition effect on the upper side of the filling body, forming an energy-gathering area. In this area, the instantaneous velocities of particles are much larger, and the stress wave is diffused in the filling body in the form of a wave. Moreover, cracks are easily formed on the interface between the ore rock and the filling body, among which the central area can be the most affected one.

(2) More specifically, the real-time monitoring of the filling body damage can be realized through the program FISH. The monitoring results indicate that: (i) to a certain extent, the filling body is damaged under the function of the blasting load, and the degree of damage is related to the distance from the blasting points; namely, the closer the distance, the higher the degree of damage, (ii) the damage on the boundary surface of the ore rock and the filling body extends and expands from the bottom to the top, which easily leads to the collapse accidents at last.

(3) With the increment of time, the energy attenuation of the stress wave in the filling body gradually becomes slower, which roughly follows the power function curve that is shaped similar to $y = ax^b$, whose coefficients 'a' and 'b' are relevant to the damping of the filling body.

(4) In terms of the software PFC, the expansive loading method of explosive point particles and the transmission boundary can substantially restore the real stope environment. In addition, to a certain extent, the damage degree of the filling body can be monitored by calling the language FISH. Above all, the research results are importantly referenced for the safety evaluation of pillar mining engineering.

Author Contributions: Resources, S.H.; Software, X.Y.; Supervision, H.Y.; Validation, X.F.; Writing—original draft, Z.X.; Writing—review & editing, H.L. All authors have read and agreed to the published version of the manuscript.

Funding: This research was funded by the National Natural Science Foundation of China, grant number 51874112, and the University Synergy Innovation Program of Anhui Province, grant number GXXT-2020-055.

Data Availability Statement: All data, models, or code that support the findings of this study are available from the corresponding author upon reasonable request.

Acknowledgments: The authors gratefully acknowledge the precious support for this research from the National Natural Science Foundation of China (Grant No.51874112), and the University Synergy Innovation Program of Anhui Province (Grant No. GXXT-2020-055).

Conflicts of Interest: The authors declare that they have no known competing financial interests or personal relationships that could have appeared to influence the work reported in this paper.

References

1. Guo, D.; Zhang, C.; Li, K. Mechanism of millisecond—Delay detonation on coal cracking under deep—Hole cumulative blasting in soft and low permeability coal seam. *J. China Coal Soc.* **2021**, *46*, 2583–2592.
2. Yang, J.; Shi, C.; Wang, S. Numerical simulation verification of blasting failure effect in rock mass with particle flow code. *J. Disaster Prev. Mitig. Eng.* **2019**, *39*, 217–226.
3. Shi, C. *Particle Flow Numerical Simulation Technology and Its Application*; Architecture & Building Press: Beijing, China, 2018.
4. Wang, B.; Cheng, P. Stress wave propagation in granular particles. *Chin. J. High Press. Phys.* **2020**, *34*, 100–107.
5. Li, X.; Tang, C. Application study on multilayer millisecond blasting mining method in small-scale open-pit quarry. *Min. Res. Dev.* **2019**, *39*, 140–143.
6. Yue, Z.; Zhang, S. Mechanism of explosive crack propagation with slotted cartridge millisecond blasting. *J. China Coal Soc.* **2018**, *43*, 638–645.
7. Yue, Z.; Zhang, S. Influence of charge structures on the slotted cartridge blasting effect. *J. Vib. Shock.* **2018**, *37*, 27–34.
8. Yue, Z.; Tian, S.; Chen, Z. Influence of the interval between holes on crack propagation in slit charge blasting. *Chin. J. Rock Mech. Eng.* **2018**, *37*, 2460–2467.
9. Guo, X.; Zhang, J. Analysis of waveform superposition in differential blasting. *Blasting* **2006**, *2*, 4–8.
10. Wu, L.; Li, H.; Nie, H. Experimental Study on the Effect of Millisecond Delay Time on Rock Fragmentation. *Initiat. Pyrotech.* **2020**, *4*, 52–56.
11. Xiang, Z.; Yang, S. The Determination of between- holes millisecond time based on blasting vibration. *China Minig Mag.* **2019**, *28*, 123–127.
12. Lou, X.; Zhou, W.; Jian, W. Millisecond blasting optimal time delay control based on rock breaking mechanism. *Journal Harbin Inst. Technol.* **2017**, *49*, 158–163.
13. Grady, D.E.; Kipp, M.L. Continuum modeling of explosive fracture in oil shale. *Int. J. Rock Mech. Min. Sci. Geomech. Abstr.* **1980**, *17*, 147–157. [[CrossRef](#)]
14. Taylor, L.M.; Chen, E.P.; Kuszmaul, J.S. Microcrack induced damage accumulation in brittle rock under dynamic loading. *Comput. Methods Appl. Mech. Eng.* **1986**, *55*, 301–320. [[CrossRef](#)]
15. Kuszmaul, J.S. A new constitution model for fragmentation of rock under dynamic loading. In Proceedings of the 2nd International Symposium on Rock Fragmentation by Blasting, Keystone, CO, USA, 23–26 August 1987; pp. 412–423.
16. Thome, B.J.; Hommert, P.J.; Brown, B. Experimental and computational investigation of the fundamental mechanisms of cratering. In Proceedings of the 2nd International Symposium on Rock Fragmentation by Blasting, Brisbane, Australia, 26–31 August 1990; pp. 117–124.
17. Yang, R.; Brwden, W.F.; Katsabanis, P.D. A new constitutive model for blast damage. *Int. J. Rock Mech. Min. Sci. Geomech. Abstr.* **1996**, *33*, 344–349. [[CrossRef](#)]
18. Liu, L.Q.; Katsabanis, P.D. Development of a continuum damage model for blasting analysis. *Int. J. Rock Mech. Min. Sci. Geomech. Abstr.* **1997**, *34*, 217–231. [[CrossRef](#)]
19. Song, J.; Kim, K. Micromechanical modeling of the dynamic fracture process during rock blasting. *Int. J. Rock Mech. Min. Sci. Geomech. Abstr.* **1996**, *33*, 387–394. [[CrossRef](#)]
20. Lu, W. *Study on Stress Wave Propagation and Its Effect in Rock Blasting*; Wuhan University: Wuhan, China, 1994.
21. Yang, J.; Wang, S. Study on fractal damage model of rock fragmentation by blasting. *Explos. Shock. Waves* **1996**, *16*, 4–10.
22. Yu, C.; Li, L.Z.; Huang, Y.M. Studies on JWL Equation of State of State of Detonation Product for Aluminized Explosive. *Explos. Shock. Wave* **1999**, *19*, 274–279.
23. Colagrossi, A.; Landrini, M. Numerical simulation of interfacialflows by smoothed particle hydrodynamics. *J. Comput. Phys.* **2003**, *191*, 448–475. [[CrossRef](#)]
24. Sadovsky, M.A.; Nersesov, I.L. Forecasts of earthquakes on the basis of complex geophysical features. *Tectonophysics* **1974**, *23*, 247–255. [[CrossRef](#)]
25. Shi, T.; Li, B. Influence of difference interval time, charge distribution and ranging on blasting vibration. *Eng. Blasting* **2003**, *4*, 10–13.

26. Hu, Y.; Lu, W.; Chen, M. Numerical simulation of the complete rock blasting response by SPH–DAM–FEM approach. *Simul. Model. Pract. Theory* **2015**, *56*, 55–68. [[CrossRef](#)]
27. Cui, T.; Ma, Y.; Wang, L. Blasting Process Simulation and Stability Study of an Open Mine Slope Based on PFC^{3D}. *Appl. Math. Mech.* **2014**, *35*, 759–767.
28. Wu, T.; Wang, K.; Ni, R. Study on calculating models of interval time in millisecond blasting. *Eng. Blasting* **1997**, *4*, 59–62.